16th World Conference on Earthquake Engineering, 16WCEE 2017
Santiago Chile, January 9th to 13th 2017
Paper N°4590 (Abstract ID)
Registration Code: S-T1464694078

CHARACTERISTICS OF STRONG GROUND MOTION IN THE KATHMANDU VALLEY DURING THE 2015 GORKHA, NEPAL EARTHQUAKE

N. Takai [1], M. Shigefuji [2], S. Bijukchhen [3], M. Ichiyanagi [4], T. Sasatani [5]

(1) Associate Prof., Hokkaido University, tki@eng.hokudai.ac.jp
(2) Assistant Prof., Kyushu University, shigefuji@arch.kyushu-u.ac.jp
(3) Graduate Student, Hokkaido University, subeg@eng.hokudai.ac.jp
(4) Technical Specialist, Hokkaido University, ichimasa@mail.sci.hokudai.ac.jp
(5) Former Prof., Hokkaido University, sasatani@eng.hokudai.ac.jp

Abstract

On 25 April 2015, a large interplate earthquake Mw 7.8 occurred in the Himalayan Range of Nepal. The focal area estimated was about 200 km long and 150 km wide, with a large slip area under the Kathmandu Valley where our strong motion observation stations were installed.

Kathmandu is the capital of Nepal and is located in the Kathmandu Valley, which is formed by soft lake sediments of Plio-Pleistocene origin. Large earthquakes in the past have caused significant damage as the seismic waves were amplified in the soft sediments. Four stations were installed along a west-to-east profile of the valley at KTP (Kirtipur), TVU (Kirtipur), PTN (Patan) and THM (Thimi); KTP is a rock site and the others are sedimentary sites.

The strong ground motions were observed during this large damaging earthquake. The maximum horizontal peak ground acceleration at the rock site was 271 cm/s^2, and the maximum horizontal peak ground velocity at the sedimentary sites reached 112 cm/s. We found while the peak accelerations were smaller than the predicted values, the peak velocities were approximately the same as the predicted values.

The horizontal components were rotated to N207E and N117E directions. The velocity waveforms at KTP showed about 6 s triangular pulses on the N207E and the UD components; however the N117E component was not a triangular pulse but a single-cycle sinusoidal wave. This distinguishing 6 s triangular pulses can be predicted by the regression model of “Fling-Step Pulse”.

The derived displacements at KTP are characterized by a monotonic step on the N207E and UD components. The vector sum of these displacement waveforms is 147 cm. Inside the Kathmandu Valley, the 163 cm vector-sum deformation and the same moving direction as the USGS fault normal direction (N205E) were obtained from GPS data. Our results derived from the KTP acceleration records are consistent with these observations.

The vertical ground velocities observed at the sedimentary sites have also the same pulse motions as observed on the rock site. On the contrary, the horizontal ground velocities (also accelerations) at the sedimentary sites have a long duration with conspicuous long-period oscillations; these are effect of the horizontal valley response. The horizontal valley response is characterized by large amplification and prolongation of oscillations. However, the predominant period and envelope shape of their oscillation differ from site to site; these features demonstrate that the long-period valley response of the Kathmandu Valley is considerably complicated.

Considering geological formations in and around the Kathmandu Valley, we may expect that the maximum horizontal peak ground acceleration is observed at the sedimentary site. However, the peak ground acceleration was recorded at the rock site KTP; this acceleration was given by isolated large ground acceleration. Finally we make a preliminary examination of the nature of the isolated large ground acceleration.

Keywords: 2015 Gorkha Earthquake, the Kathmandu Valley, Strong Ground Motion, Valley response, Velocity pulse

1. Introduction

The Himalayan mountain range formed by the collision of the Indian and Eurasian plates is regarded as one of the earthquake prone zones in the world. The Indian Plate underthrusts the Eurasian Plate and a number of large earthquakes have occurred in Nepal Himalaya. Kathmandu is the capital of Nepal and is located on the Kathmandu Valley. The Valley is surrounded by mountains on all sides and is filled with soft lake sediments of Plio-Pleistocene origin [1]; the thickness of the sediments is more than 500 m at the central part of the valley. Large earthquakes in the past have caused significant damage in the Kathmandu Valley; in case of the 1934 Nepal-Bihar earthquake (Mw 8.2), nearly 19 % of buildings were destroyed inside the Valley and more than 8,000 people lost their life all over the country [2]. A principal factor in the significant damage is considered to be effect of the soft lake sediments on seismic motion. Considering these tectonic and site conditions of the Kathmandu Valley, we have started a strong motion array observation (four sites; one rock site and three sedimentary sites) in the Valley, on 20 September 2011, to understand the site effects of the Kathmandu Valley on strong ground motion.

On 25 April 2015, a large earthquake of Mw 7.8 occurred along the Himalayan front. This event has a low-angle thrust faulting mechanism and the 8.2 km hypocentral depth [3]. The epicenter is near the Gorkha region, 80 km north-west of the Kathmandu Valley, while the source area propagated eastward, passing the Kathmandu Valley [3-7]. This event resulted in over 8,000 deaths, mostly in the Kathmandu and adjacent districts [8]. We succeeded in observing strong ground motions at our array sites in the Kathmandu Valley during this devastating earthquake.

In this article we describe characteristics of ground motions observed in the Kathmandu Valley and a preliminary examination of the slip pulse and isolated large ground acceleration only recorded at the rock site. Data used in this article include the ground motions observed by the Faculty of Engineering, Hokkaido University in collaboration with the Central Department of Geology, Tribhuvan University, Nepal, also those observed by USGS [9] and high-rate GPS data recorded by UNAVCO [7].

2. Strong Ground Motion Observation

Accelerometers have been installed at four sites along the straight (west-to-east) profile in the Valley: the sites are KTP (Kirtipur), TVU (Kirtipur), PTN (Patan) and THM (Thimi) as shown in Fig. 1. We are using highly damped moving coil type Mitsutoyo JEP-6A3-2 accelerometers [10] and Hakusan DATAMARK LS-8800 data loggers with GPS time calibration. The accelerometer has a flat response (-3 dB) of ground acceleration from 0.1 Hz to an aliasing frequency. It is necessary to apply a correction of the sensor-response to the observed records in order to derive true ground motions[10].

The surface (~ 20 m) S-wave velocities of the observation sites were investigated by the surface wave method when we installed the instruments [11]. The velocity of S-wave is over 700 m/s at the KTP site, but it is less than 200 m/s at the other three sites. These velocities are consistent with the geological formations; KTP is located on rock and TVU, PTN and THM are located on the lake sediment of the valley (Fig. 1). The detail of this array network system and data processing were described in Takai *et al.* [12].

3. Overview of Strong Ground Motion Records

3.1 Ground accelerations

The focal area of the 2015 Gorkha earthquake estimated by USGS [3] is about 200 km long and 150 km wide (Figure 1b), with a large slip area near the Kathmandu Valley. During data processing, first we made a base-line correction by removing the mean determined from a segment of the pre-event part of the original record from the whole original acceleration record. Next we applied the sensor-response correction in the frequency domain by using FFT. Next, we derived the velocity and displacement waveforms from the sensor-response corrected accelerograms by integration in the time domain. Finally, the horizontal components were rotated in the N207E and N117E directions; the rotation angle was that one of the horizontal components at KTP yields the maximum horizontal displacement at the end of shaking. The N207E and N117E directions are nearly the same as the opposite to fault dip direction (N205E) and the opposite direction of fault strike (N115E) directions of the

USGS fault plane [3]. In this paper, we show the whole records using the N117E, N207E, and UD coordinate system.

The accelerograms obtained after applying the sensor-response correction and rotating the horizontal components are shown in Fig. 2 along with that of the KATNP station achieved by USGS. The largest peak ground acceleration (PGA: 246 cm/s^2) is recorded on the N117E component at the rock site KTP, and the vector sum of the horizontal components is 255 cm/s^2 at this station. This large PGA is given by isolated large ground acceleration at about 28 s from the origin time. The horizontal PGA values are compared with those predicted by the ground motion prediction equation (GMPE; [14]) for ground accelerations. We find the observed PGA values are smaller than those estimated by the GMPE [14]; the average of the observed PGAs is less than one-third of the predicted PGA (Fig. 3). One cause of the low PGA on sedimentary basin might be considered the nonlinear soil response[15]. However, we have not grasped the cause of this including Q of this area and source characteristics completely.

The horizontal accelerograms at the sedimentary sites have a long duration with conspicuous long-period oscillations; however, the envelopes of the oscillations differ from site to site. On the other hand, the vertical accelerograms at all the sites are nearly the same and have no long-period oscillations. These characteristics demonstrate the site effects of the Kathmandu Valley, that is, the valley response.

These conspicuous long-period accelerations were also observed on the lake zone in Mexico City during the 1985 Michoacan earthquake (Mw 8.0) [16]. Both the PGA values are comparable, while the predominant periods are somewhat different; the periods in the Kathmandu Valley are 3 to 5 s (also see Fig. 4) and those in Mexico City are 2 to 3 s. We should note that although both the conspicuous long-period accelerations are effect of the lake sediments under the valleys, the exciting mechanism may be different because the distance from the source area to the Kathmandu Valley is about 10 km, while the distance to Mexico City is about 300 km; therefore, the incoming wave-fields into both the valleys are different from each other.

It is well known that the long-period accelerations collapsed or severely damaged many tall buildings in

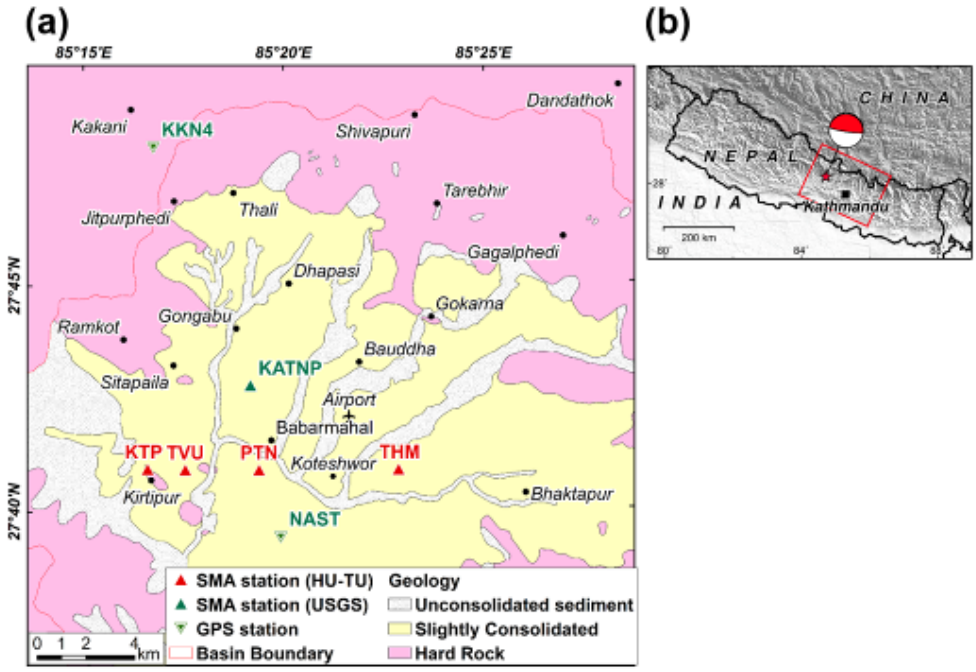

Fig. 1 Location map of strong motion stations.
a) Observation sites in the Kathmandu Valley with geological formations (modified from Shrestha et al. [13]). Strong motion accelerometer (SMA) stations are divided to HU-TU: Hokkaido University and Tribhuvan University, and USGS sites. GPS stations are used in Galetzka et al. [7].
b) The epicenter of the 2015 Gorkha earthquake is shown by the red star. The fault plane estimated by USGS [3] is shown with the red rectangular. A beach ball is the focal mechanism by USGS [3].

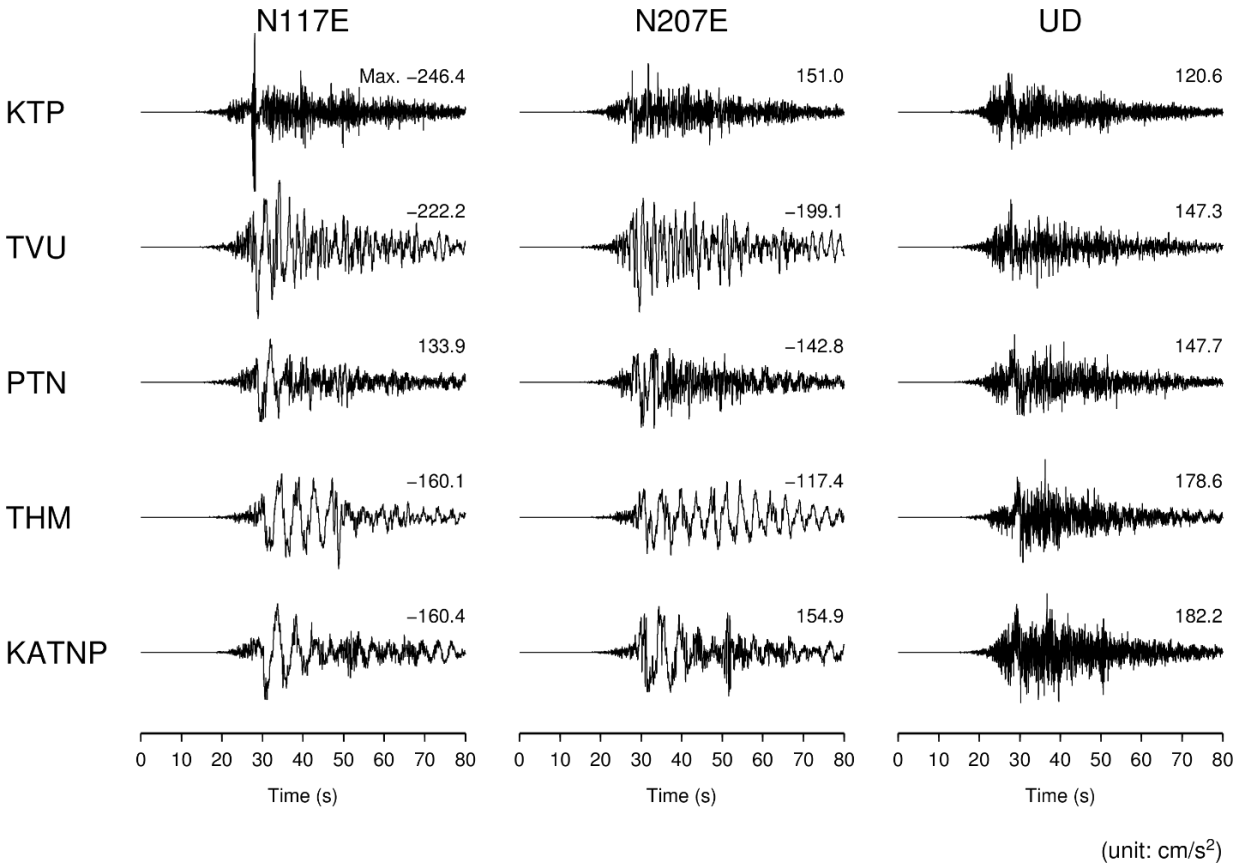

the lake zone in Mexico City [16]. Fortunately, in case of the Gorkha earthquake, there were no high-rise or base isolated buildings with the long natural period in the Kathmandu Valley.

Fig. 2 Observed ground accelerations at five stations during the 2015-04-25 Gorkha EQ. The horizontal components are rotated ones; the rotation angle is that one of the horizontal components at KTP yields the maximum horizontal displacement at the end of shaking (see Fig. 5). According to the USGS fault model [3], the N117E and N207E directions nearly correspond to the opposite direction of fault strike and opposite to fault dip direction, respectively.

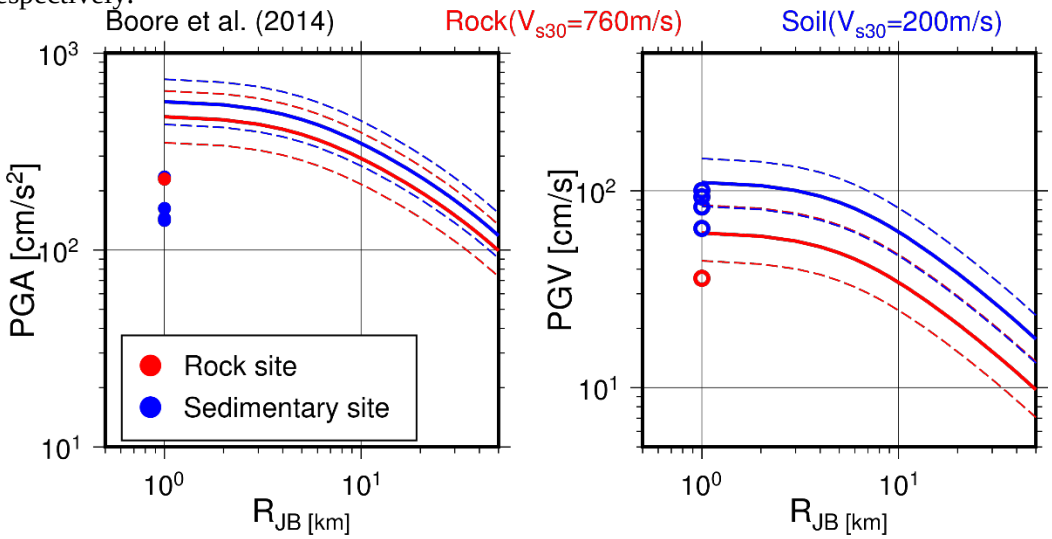

Fig. 3 Comparison between the observed and predicted PGAs (Left) and PGVs (Right); the predicted ones were obtained by using GMPE[14]. The solid red lines indicate rock site (V_{S30} = 760 m/s) with standard error (dashed lines). The solid blue lines indicate soil site (V_{S30} = 200 m/s) with standard error (dashed lines). Distance R_{JB} means closest distance to the surface projection of the fault plane, therefore, 0 km (Kathmandu valley placed on the fault plane) are replaced to 1 km in the figures.

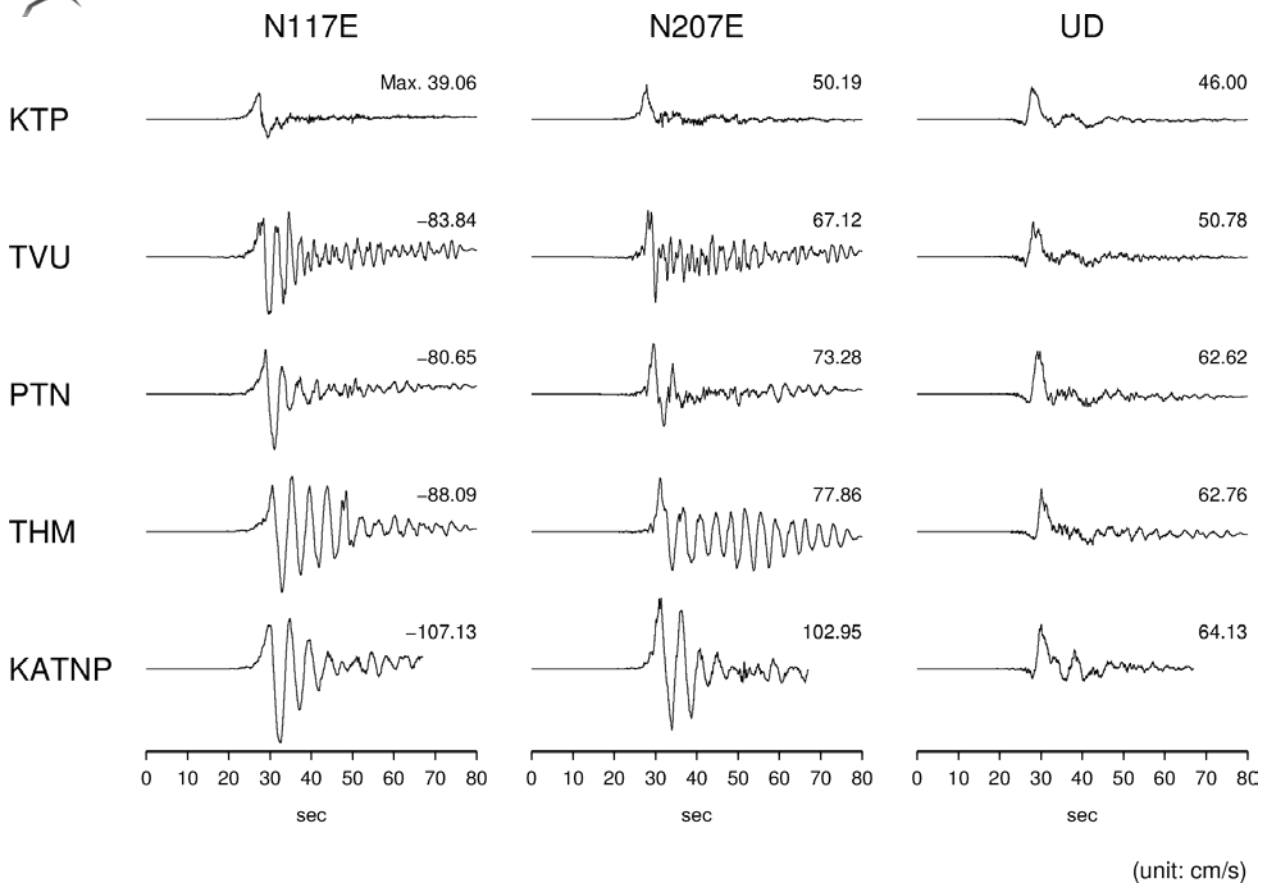

Fig. 4 Ground velocities at five stations. The N117E and N207E are the fault parallel and fault normal components, respectively.

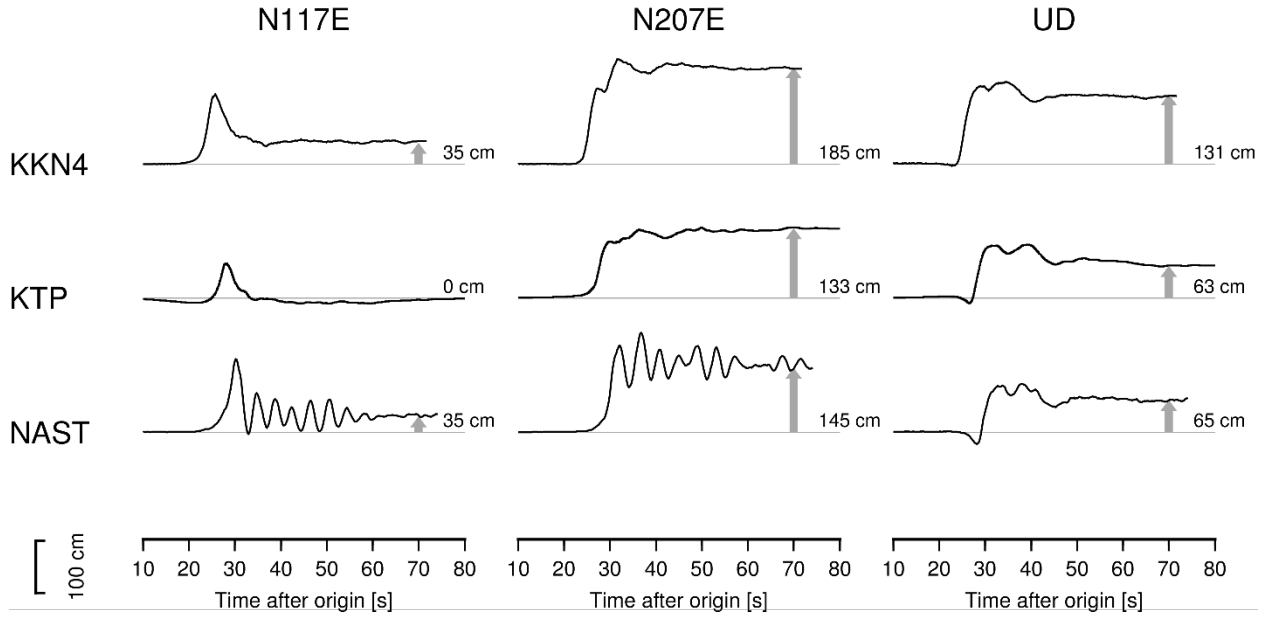

Fig. 5 Ground displacement at the rock site KTP. The N117E and N207E are the fault parallel and fault normal components, respectively. The KKN4 and NAST ground displacements were obtained by GPS records; these were obtained from UNAVCO [7].

3.2 Ground velocities

The highest peak ground velocity 107 cm/s (the vector sum of the horizontal components) is given at TVU. We compare the observed PGV values with those predicted by the GMPE as the same manner for the PGA values. While the observed PGA values are much smaller than the predicted ones, the observed PGV values are a bit smaller than the predicted ones at the sedimentary stations (Fig. 3).

The UD component ground velocities at the sedimentary sites are nearly the same as that observed at the rock site KTP. On the contrary, the horizontal ground velocities at the sedimentary sites have a long duration with conspicuous long-period oscillations. When we assume the KTP (rock site) ground velocities are the incoming wave fields into the Kathmandu Valley, we may consider the large ground velocities on the sedimentary sites in Fig. 4 to be the long-period (3~5 s) valley response. Takai *et al.* [12] compared the Fourier amplitude spectral ratios of the sedimentary site spectra to the rock site spectrum for each component, and pointed out that the long-period valley response of the Kathmandu Valley is considerably complicated. Furthermore, the site effect of deep underground velocity structure were discussed preliminary with aftershocks data [17, 18]

The velocity waveforms on the N207E and UD components observed at the rock site KTP show the distinguishing velocity pulse ground motions; the arrival time of the velocity pulses roughly corresponds to the S-wave arrival time from the hypocenter. They show a single-sided velocity pulse with a width of about 6 s, while the N117E component show a double-sided pulse with a period of about 10 s. The ground velocities at KKN4 obtained from the high-rate (5 Hz sampling) GPS record [7] have the similar waveforms as observed at KTP, while the amplitudes of the KKN4 velocity pulses are about 1.4 times larger than those of the KTP velocity pulses; KKN4 is a rock site located northwest of the Kathmandu Valley as shown in Fig. 1.

3.3 Ground displacements

The ground velocities at KTP where the simple velocity pulses are observed are integrated to derive the displacement waveforms. The KTP displacement waveforms are shown in Fig. 5, together with those observed by the high-rate GPSs at KKN4 and NAST [7]; these locations are shown in Fig. 1.

The derived displacements at KTP are characterized by a monotonic step, also including the contributions of dynamic phases, on the fault-normal and UD components. They show permanent displacements of 133 cm in the fault-normal direction and 63 cm in the upward direction; the vector sum is 147 cm, while there is negligible permanent displacement in the fault-parallel direction.

The displacement waveforms at KTP are similar to those at the rock site KKN4 for the three components. However, their permanent deformation values are different; the values at KKN4 are larger than those at KTP because the KKN4 site is more near the large slip area [7]. The UD displacement and permanent deformation at the sedimentary site NAST are similar to those at KTP. However, the horizontal displacement waveforms at NAST are different from those at KTP; the long-period oscillations observed at NAST result from the valley response as mentioned in the previous section. In spite of the contamination by the valley response, the horizontal permanent deformation values at NAST are nearly the same as those at KTP; the distance between NAST and KTP is only 6 km. These evidences indicate that the displacement waveforms at KTP derived from the accelerograms give the reliable motion of the Earth's surface.

4. Effect of Permanent Tectonic Offset on Strong Ground Motions

The velocity pulse and pulse-like ground motions observed near surface faults are considered to be effect of forward rupture directivity or a permanent tectonic offset [e.g., 19, 20-23]. The Kathmandu Valley is located at a very close distance (~10 km) to the rupture area and the estimated large slip areas exist near the valley [7]. Furthermore, the displacement waveforms derived from the velocity pulses on the N207E and UD components show a monotonic step as shown in Fig. 5. These facts demonstrate the observed velocity pulses are effect of a permanent tectonic offset [19]. On the other hand, the N117E component at KTP shows clear double-sided pulse on the velocity waveform. This pulse is considered to be effect of along-strike directivity [19], and the pulse shape was explained by the joint inversion result for rupture process [24].

The distinguishing KTP velocity pulses may be assumed to be the "Fling-Step" motion [21, 25]. Recently Kamai *et al.* [25] developed an updated parametric model for the fling-step components based on an extensive

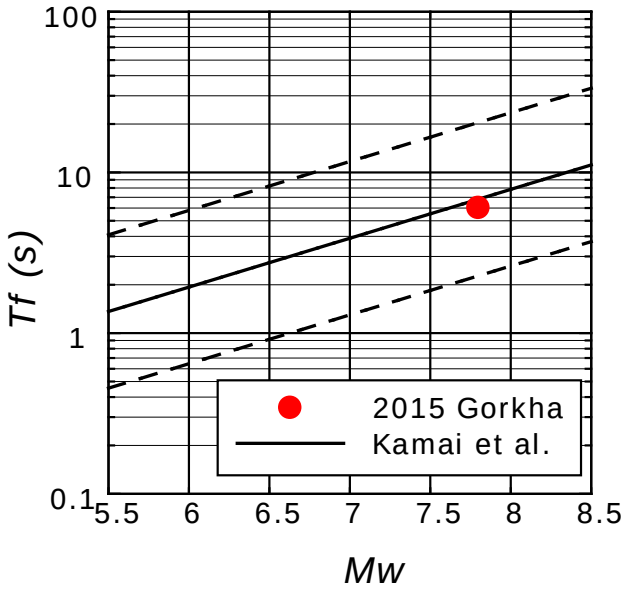

Fig. 6 Comparison of the width of the velocity pulse observed at KTP with the regression model of the period of the fling-step pulse for the reverse fault by Kamai *et al.* [25] . Medians are shown by a solid line and confidence intervals, by the dashed lines.

set of finite-fault simulations. Their three fling-step parameters are the fling-step amplitude, the period of the fling-step pulse (this parameter corresponds to a width of the velocity pulse), and the onset time of the fling step pulse.

Here we compare the width of the velocity pulse observed at KTP with their regression model of the period of the fling-step pulse for the reverse fault. As mentioned in the 3.2 section, the width of velocity pulses at KTP is about 6 s. This value is nearly the same as the median value of the regression model by Kamai *et al.* [25] as shown in Fig. 6. This means that the Gorkha earthquake with Mw 7.8 is normal one with respect to the fling-step motion.

As shown in Fig. 4, the horizontal long-period ground motions, the fling-step pulse (N207E) and the along-strike directivity pulse (N117E), observed at the rock site KTP were strongly amplified and elongated on the sedimentary sites; that is, the long-period valley response. Takai *et al.* [12] calculated horizontal velocity response spectra (h=0.05) for the horizontal ground motions shown in Fig. 4 to discuss their destructive power for buildings. They concluded that the horizontal long-period oscillations on the sedimentary sites had enough destructive power to damage high-rise buildings which have natural periods of 3 to 5 s.

5. Isolated Large Ground Acceleration at the Rock Site KTP

Considering geological formations in and around the Kathmandu Valley (Fig. 1), we may expect that the largest PGA is observed at the sedimentary site. In the 3.1 section, however, we pointed out that the largest PGA was recorded on the N117E component at the rock site KTP (Fig. 2). This PGA was given by isolated large ground acceleration at about 28 s from the origin time; the acceleration appears as a spike on the time scale used in Fig. 2. We make a preliminary examination of the nature of the isolated large ground acceleration based on the enlarged time-scale acceleration time histories.

First, we compare the three-component acceleration time histories at the KTP site and their Fourier spectra for the short time window which include the isolated large ground acceleration on the N117E component (Fig. 7). The predominant frequency of the isolated large ground acceleration on the N117E component, which lasted for about 1 s, is about 4 Hz. The other components, however, have no this predominant frequency. This means the particle motion of the isolated large ground acceleration is polarized into the N117E direction.

Next, we compare the N117E-component acceleration time histories at our array sites; the rock site KTP and three sedimentary sites (Fig. 8). Figure 8 clearly shows strong amplification of the long-period (3-5 s) accelerations at the sedimentary site; that is, the long-period valley response which has been discussed based on

the ground velocities in the 3.2 section. However we cannot identify the isolated large ground acceleration on the acceleration time histories at the sedimentary sites. This disappearance of the isolated large ground acceleration at

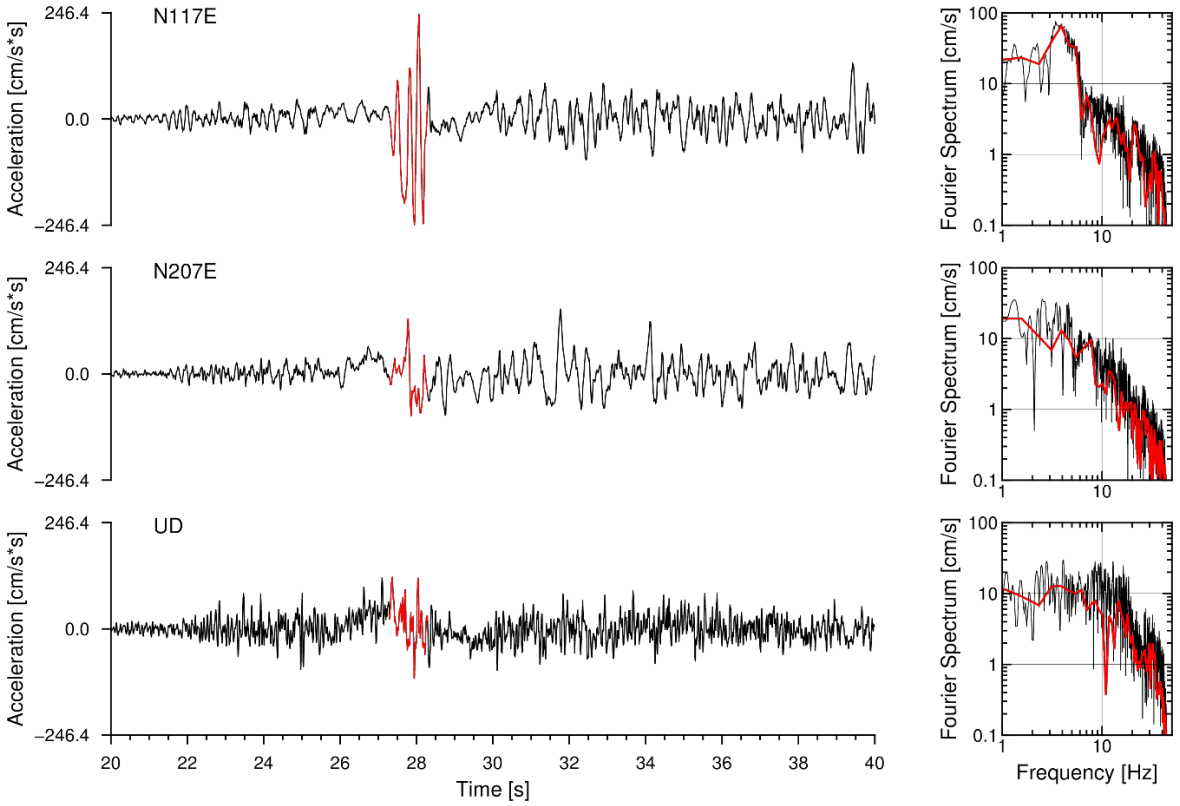

Fig. 7 Observed three-component ground accelerations (left) and their Fourier spectra (right) at KTP. A red section on each component is the time window for red line Fourier spectra.

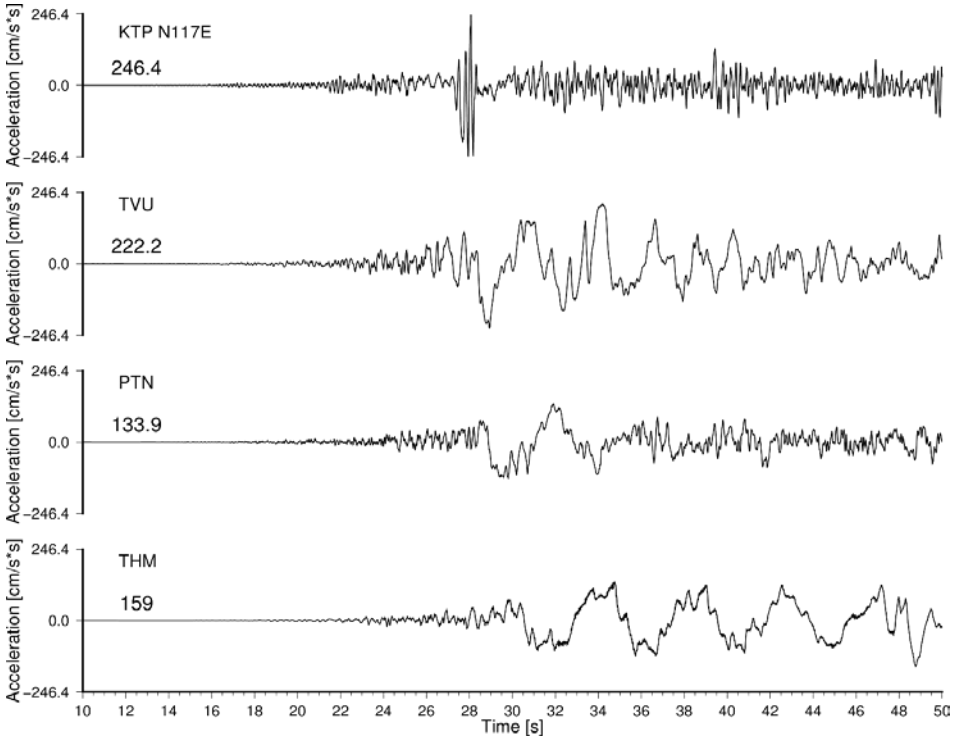

Fig. 8 Comparison of the N117E-component accelerations at our array stations. Note that the acceleration time histories are shown in enlarged time scale.

the sedimentary sites may result from nonlinear soil response induced by large peak horizontal ground velocities (70 - 90 cm/s); the nonlinear soil response resulted in the reduced amplitudes of short-period ground motions.

It is interesting to consider the excitation mechanism of the isolated large ground acceleration observed at KTP. Since the instruments are covered with wooden box, it is not considered to be potentially the isolated peak associated with some falling objects. In addition, 4 Hz are relatively low for the cause of the falling objects effects. The isolated large ground acceleration appeared at nearly the same time when the large (~40cm/s) velocity pulse arrived at KTP (see Fig. 4). This may suggest that dynamic stress carried by the large velocity pulse triggered a small event around the main fault plane beneath KTP. The Fourier spectrum of whole part on N117E component are strongly affected by this isolated large ground acceleration; short period strong motion is characterized by this isolated large ground acceleration at KTP. However, since the observed record of the isolated large ground acceleration is only one, it is difficult to confirm this excitation mechanism anyway.

6. Concluding Remarks

Since the capital city of Nepal, Kathmandu, on the sediment-filled valley, was located at a very close distance to the fault plane of the 2015 Gorkha earthquake, a wealth of new strong ground motions was obtained there. On the rock sites, the simple velocity pulses were observed on the fault normal and vertical components; they are effect of a permanent tectonic offset. On the sedimentary sites, although the velocity pulses were also observed on the vertical component, the horizontal ground velocities showed largely amplified and prolonged long-period oscillations compared with the rock site motions; these resulted from the valley response. Since the horizontal long-period oscillations have enough destructive power to damage high-rise buildings, it is important for us to understand the factors in the long-period valley response observed in the Kathmandu valley based on the 3-D velocity structure of the valley.

7. Acknowledgements

The KATNP record was provided by USGS [9]. The KKN4 and NAST data were obtained from UNAVCO website [7]. A part of this study was supported by the Grant-in-Aid for Scientific Research No. 23404005 and 15H05793 from MEXT of Japan, Heiwa Nakajima Foundation, Obayashi Foundation, MEXT of Japan's Earthquake and Volcano Hazards Observation and Research Program, JST of Japan's J-RAPID Program, and JICA-JST SATREPS Program. Grateful thanks to Dr. MR. Dhital, Y. Dhakal, S. Ghimire, Messrs. S. Rajaure, K. Sawada, H. Okajima, Y. Miyahara and M. Aoki. We used the Generic Mapping Tools [26] for drawing the part of the figures.

8. References

[1] Dhital M R (2015): Geology of the Nepal Himalaya. 1 edn. Springer International Publishing, Switzerland. doi:10.1007/978-3-319-02496-7

[2] Dixit A M, Yatabe R, Dahal R K, Bhandary N P (2013): Initiatives for earthquake disaster risk management in the Kathmandu valley, Natural Hazards, 69, 631-654.

[3] Usgs (2015): M7.8 - 36km E of Khudi, Nepal. http://earthquake.usgs.gov/earthquakes/eventpage/us20002926#scientific_finitefault:us_us20002926. Accessed SEP20 2015.

[4] Yagi Y, Okuwaki R (2015): Integrated seismic source model of the 2015 Gorkha, Nepal, earthquake, Geophysical Research Letters, 42, 2015GL064995.

[5] Avouac J P, Meng L, Wei S, Wang T, Ampuero J P (2015): Lower edge of locked Main Himalayan Thrust unzipped by the 2015 Gorkha earthquake, Nature Geoscience, 8, 708-711.

[6] Fan W Y, Shearer P M (2015): Detailed rupture imaging of the 25 April 2015 Nepal earthquake using teleseismic P waves, Geophysical Research Letters, 42, 5744-5752.

[7] Galetzka J, Melgar D, Genrich J F, Geng J, Owen S, Lindsey E O, Xu X, Bock Y, Avouac J P, Adhikari L B, Upreti B N, Pratt-Sitaula B, Bhattarai T N, Sitaula B P, Moore A, Hudnut K W, Szeliga W, Normandeau J, Fend M, Flouzat M, Bollinger L, Shrestha P, Koirala B, Gautam U, Bhatterai M, Gupta R , Kandel T, Timsina C, Sapkota S N, Rajaure S, Maharjan N (2015) : Slip pulse and resonance of the Kathmandu basin during the 2015 Gorkha earthquake, Nepal, Science, 349, 1091-1095.

[8] Moha (2015): The Ministry of Home Affairs (MoHA) Government of Nepal: Nepal Earthquake 2015: Disaster Recovery and Reconstruction Information Platform (NDRRIP). http://drrportal.gov.np/ndrrip/main.html. Accessed OCT 20 2015.

[9] Usgs (2015): NetQuakes:Station KATNP_NQ_01, 25 April 2015. http://earthquake.usgs.gov/monitoring/netquakes/station/KATNP_NQ_01/20150425061138/. Accessed SEP20 2015.

[10] Kudo K, Kanno T, Okada H, Özel O, Erdik M, Sasatani T, Higashi S, Takahashi M, Yoshida K (2002) : Site-specific issues for strong ground motions during the Kocaeli, Turkey, earthquake of 17 August 1999, as inferred from array observations of microtremors and aftershocks, Bulletin of the Seismological Society of America, 92, 448-465.

[11] Takai N, Sawada K, Shigefuji M, Bijukchhen S, Ichiyanagi M, Sasatani T, Dhakal P, Rajaure S, Dhital M R (2015) : Shallow underground structure of strong ground motion observation sites in the Kathmandu valley, Journal of Nepal Geological Society, 48, 50-50.

[12] Takai N, Shigefuji M, Rajaure S, Bijukchhen S, Ichiyanagi M, Dhital M, Sasatani T (2016) : Strong ground motion in the Kathmandu Valley during the 2015 Gorkha, Nepal, earthquake, Earth, Planets and Space, 68, 10.

[13] Shrestha O, Koirala A, Karmacharya S, Pradhananga U, Pradhan P, Karmacharya R (1998) Engineering and environmental geological map of the Kathmandu valley. Department of Mines and Geology, Kathmandu.

[14] Boore D M, Stewart J P, Seyhan E, Atkinson G M (2014) : NGA-West2 equations for predicting PGA, PGV, and 5% damped PSA for shallow crustal earthquakes, Earthquake Spectra, 30, 1057-1085.

[15] Rajaure S, Asimaki D, Thompson E M, Hough S, Martin S, Ampuero J P, Dhital M R, Inbal A, Takai N, Shigefuji M, Bijukchhen S, Ichiyanagi M, Sasatani T, Paudel L ((In press)) : Characterizing the Kathmandu Valley sediment response through strong motion recordings of the 2015 Gorkha earthquake sequence, Tectonophysics.

[16] Anderson J G, Bodin P, Brune J N, Prince J, Singh S K, Quaas R, Onate M (1986) : Strong ground motion from the Michoacan, Mexico, earthquake, Science, 233, 1043-1049.

[17] Shigefuji M, Takai N, Bijukchhen S, Ichiyanagi M, Sasatani T (2016) : Characteristics of Long-Period Ground Motion in the Kathmandu Valley from the Large Aftershocks of the 2015 Gorkha Nepal Earthquake, 5th IASPEI / IAEE International Symposium: Effects of Surface Geology on Seismic Motion.

[18] Bijukchhen S, Takai N, Shigefuji M, Ichiyanagi M, Sasatani T (2016) : Trial Construction of 1-Dvelocity Structure of the Kathmandu Valley Using the Medium and Large Earthquake Records, 5th IASPEI / IAEE International Symposium: Effects of Surface Geology on Seismic Motion.

[19] Mavroeidis G P, Papageorgiou A S (2003) : A mathematical representation of near-fault ground motions, Bulletin of the Seismological Society of America, 93, 1099-1131.

[20] Loh C-H, Lee Z-K, Wu T-C, Peng S-Y (2000) : Ground motion characteristics of the Chi-Chi earthquake of 21 September 1999, Earthquake Engineering & Structural Dynamics, 29, 867-897.

[21] Hisada Y, Bielak J (2003) : A Theoretical Method for Computing Near-Fault Ground Motions in Layered Half-Spaces Considering Static Offset Due to Surface Faulting, with a Physical Interpretation of Fling Step and Rupture Directivity, Bulletin of the Seismological Society of America, 93, 1154-1168.

[22] Dreger D, Hurtado G, Chopra A, Larsen S (2011) : Near-field across-fault seismic ground motions, Bulletin of the Seismological Society of America, 101, 202-221.

[23] Baker J W (2007)：Quantitative classification of near-fault ground motions using wavelet analysis，Bulletin of the Seismological Society of America，97，1486-1501.

[24] Kobayashi H，Koketsu K，Miyake H，Takai N，Shigefuji M，Bhattarai M，Sapkota S N (2016)：Joint inversion of teleseismic, geodetic, and near-field waveform datasets for rupture process of the 2015 Gorkha, Nepal, earthquake ，Earth, Planets and Space，68，1-8.

[25] Kamai R，Abrahamson N，Graves R (2014)：Adding Fling Effects to Processed Ground-Motion Time Histories, Bulletin of the Seismological Society of America，104，1914-1929.

[26] Wessel P，Smith W H F (1991)：Free software helps map and display data，Eos, Transactions American Geophysical Union，72，441-441.